Photoinduced production of substances with humic-like fluorescence, upon irradiation of water samples from Alpine lakes

Luca Carena, Yiqun Wang, Sasho Gligorovski, Silvia Berto, Stéphane Mounier, Davide Vione

Photoinduced production of substances with humic-like fluorescence, upon irradiation of water samples from Alpine lakes

Luca Carena,[a] Yiqun Wang,[b] Sasho Gligorovski,[b,*] Silvia Berto,[a] Stéphane Mounier,[c] Davide Vione [a,*]

[a] *Dipartimento di Chimica, Università di Torino, Via Pietro Giuria 5, 10125 Torino, Italy.*

[b] *State Key Laboratory of Organic Geochemistry, Guangzhou Institute of Geochemistry, Chinese Academy of Sciences, Guangzhou 510 640, China.*

[c] *Univ. Toulon, Aix Marseille Univ., CNRS/INSU, IRD, MIO UM 110, Mediterranean Institute of Oceanography, CS 60584, 83041 – Toulon, France.*

* Correspondence: *gligorovski@gig.ac.cn* (SG), *davide.vione@unito.it* (DV)

Abstract

Evidence is here provided that irradiation of some lake water samples can trigger the formation of fluorophores with humic-like properties, at the same time increasing water absorbance. This phenomenon is the opposite of photobleaching, which is often observed when natural waters are irradiated. Photogeneration of humic-like compounds can be highlighted in water samples where the initial fluorescence signal of humic substances is low, so that photobleaching is minimised. Samples that are most likely to show photoinduced formation of humic-like fluorophores are in fact characterised by high values of protein-like vs. humic-like contribution ratios to fluorescence, as evidenced by parallel factor (PARAFAC) analysis. Mountain lakes in late summer appear to be suitable candidates to highlight the described phenomenon. In some cases, lake-water irradiation caused a decrease in the spectral slope of the absorbance that, together with increasing absorbance values, is consistent with an increase in molecular mass and aromaticity of organic matter. The

absorbance increase triggered by irradiation might play a role in screening biologically harmful UV radiation, in mountain environments that would otherwise be characterised by very clear water, where UV light can be easily transmitted along the water column.

Keywords: Aquagenic organic matter; Photochemistry; Fluorescence; PARAFAC analysis; Spectral slope.

Introduction

Humic substances (HS) are important components of both chromophoric and fluorescent dissolved organic matter (respectively, CDOM and FDOM) in natural waters, and play important roles as metal complexing agents, radiation absorbers, and photosensitisers (Krachler and Krachler, 2021; Nelson and Siegel, 2013; Zhou et al., 2019). Interaction between HS and metals or hydrophobic pollutants contributes to keep these species dissolved, and to change their toxicity or bioavailability (De Paolis and Kukkonen, 1997; Koukal et al., 2003; Suzuki and Shoji, 2020; Worms et al., 2015). Furthermore, HS screen sunlight and they are a key factor in, among others, light penetration in the water column, thermocline depth in stratified lakes, protection of living organisms against harmful UV radiation, and contaminant degradation *via* photochemically produced reactive intermediates (Berg et al., 2019; Remucal, 2014; Zhang et al., 2014; Shank et al., 2010; Sommaruga, 2001; Sommaruga et al., 1999; Vione et al., 2014). Spectroscopic techniques (both absorption and fluorescence) are widely used for HS detection and characterisation (Coble, 1996; Galgani et al., 2011; Loiselle et al., 2009).

A major route of HS to surface waters is leaching from soil, in which case HS make up an important fraction of allochthonous organic matter (Osburn and Stedmon, 2011). Precipitation water plays key role in transferring soil HS to water basins (Nguyen et al., 2013; Tipping et al., 1999), where HS can for instance undergo photobleaching upon exposure to sunlight (Brinkmann et al., 2003; Del

Vecchio and Blough, 2002; Helms et al., 2014). Photobleaching is the loss of chromophores (and often also the fluorophores) induced by sunlight radiation, and it can be a very important transformation route for biorecalcitrant compounds like HS (Clark et al., 2019; Gu et al., 2017; Niu et al., 2014; Vähätalo and Wetzel, 2004).

The scenario is actually more complex, because HS are partially aquagenic. This means they can be formed autochthonously in natural surface waters, from a range of precursors. Recent evidence suggests that a complex network of biological and photoinduced processes may be responsible for the production and processing of fluorescent organic matter, starting from extracellular polymeric substances released by microorganisms (Fox et al., 2019; Yang et al., 2021). Aquagenic HS take part in these processes, where they are both produced and consumed (He et al., 2016; Yang et al., 2021), and where the exact roles of radiation and biological reactions are still unclear.

On the one side, photobleaching is a well-known, radiation-induced phenomenon involving HS (Dainard et al., 2015; Del Vecchio and Blough, 2002; Helms et al., 2008; Yamashita et al., 2013). On the other side, laboratory evidence suggests that compounds with HS-like properties, including HS-like fluorescence, are produced by irradiation of precursors such as amino acids (tryptophan and tyrosine) and phenols, including lignin breakdown compounds (Berto et al., 2018, 2016; Bianco et al., 2014). Photoinduced formation of humic-like substances has opposite features compared with photobleaching, because it causes an increase in long-wavelength (> 300 nm) absorbance. From a mechanistic point of view, this photochemical process could involve dimerisation/oligomerisation, as well as hydroxylation of the precursor molecules (see **Scheme S1** in the Supplementary Material, hereinafter SM, for a possible example of such processes) (De Laurentiis et al., 2013; Hoffer et al., 2004; Mabato et al., 2022). Indeed, evidence suggests that phenolic oligomers and poly-hydroxylated aromatic compounds are reasonable humic fluorophores (Vione et al., 2021).

Unfortunately, very little is currently known about the possibility that formation of HS (or otherwise, of compounds with HS-like fluorescence) may occur photochemically in real surface-water samples. The main obstacle to highlight this process is the fact that existing HS in the sample

would undergo photobleaching, thereby potentially masking possible photoinduced formation of additional HS-like compounds from non-humic precursors. Because of this problem, the ideal sample to be irradiated should initially contain little to no HS, which is not easy to be attained. However, past studies have found out that water from mountain lakes at the end of the boreal summer season (mid September) exhibits fluorescence signals that can be assigned to proteins, or even to sunlight-absorbing plankton pigments, but little to no HS fluorescence (De Laurentiis et al., 2012). In contrast, HS signals are detected in samples taken from the same lakes, soon after ice melting (mid June) (Bianco, 2013). Possible reasons for this finding are summer (June-August) photobleaching of initially-occurring HS, plus high turnover of algal cells in late summer, including important cell lysis.

Excitation-emission matrix (EEM) fluorescence spectroscopy is one of the most straightforward ways to characterise organic matter in natural water samples (Minor et al., 2014; Stedmon et al., 2003). The signals that are most often detected in EEM spectra are those of proteins and HS (Vione et al., 2021). Protein fluorescence is detected based on the main fluorophores, *i.e.* tyrosine (Ex ~ 230 nm; Em ~ 300 nm, where Ex means excitation wavelength and Em means emission wavelength), and tryptophan (Ex ~ 230 nm; Em ~ 350 nm) (Coble, 1996; Stedmon et al., 2003; Trubetskaya et al., 2016). In contrast, HS typically have two fluorescence peaks at Ex/Em = ~250/ ~450 nm, and ~320/ ~450 nm (Bridgeman et al., 2011; Coble, 1996; Stedmon et al., 2003). The presence of multiple signals in the EEM spectrum of a natural water sample may require the use of decomposition techniques to separate the different components, among which PARAllel FACtor analysis (PARAFAC), introduced by Bro (1997) and popularised by Stedmon et al. (2003) plays a major role. Indeed, spectral fluorescence data are multi-way (three-way) signals that depend on the wavelength of light absorbed (excitation) and the wavelength at which fluorescence is observed (emission). These data enter in a data cube that the PARAFAC algorithm fits by minimising difference between the three-way model parameters (emission, excitation, and

contribution) and the observed signals that constitute the Excitation-Emission Matrices of fluorescence (EEMs) (Andersen and Bro, 2003; Cory and McKnight, 2005; Murphy et al., 2013).

In this context, this work has the goal of figuring out if compounds with humic-like fluorescence can actually be formed upon irradiation of samples of natural surface water. To minimise the occurrence of humic fluorescence signals in the initial samples, the latter were taken from mountain lakes in late summer. EEM spectroscopy, coupled with PARAFAC analysis, was mainly used to monitor changes in fluorescent organic matter in the investigated samples.

Materials and methods

Alpine lakes under study

The study lakes are located in the north-western part of the Italian Alps, in the Piedmont region (see map in **Figure 1**). In particular, Lakes Rouen, Soprano, and Sottano are located in the Orsiera-Rocciavrè Natural Park, at 2391, 2213, and 2102 m a.s.l., respectively, while Lake Rosset (2701 m a.s.l.) and the three Lakes Tre Becchi (2727 m a.s.l., hereinafter called Tre Becchi A, B, and C [A=Left; B=Central; C=Right]) are in the Gran Paradiso National Park. The lakes are small and shallow, all located above the tree line, and mainly surrounded by rocks and grasses. During sampling (mid-September 2018, *i.e.*, late boreal summer), the surface of the lakes was completely ice-free.

Water samples (1 L from each lake) were kept refrigerated and in the dark during transport to the laboratory, where they were vacuum-filtered with polyamide filters (0.45 mm pore size, Sartorius). In order to prevent modifications caused by residual biological activity, the filtered samples were kept in the dark at ~5 °C till the irradiation experiments.

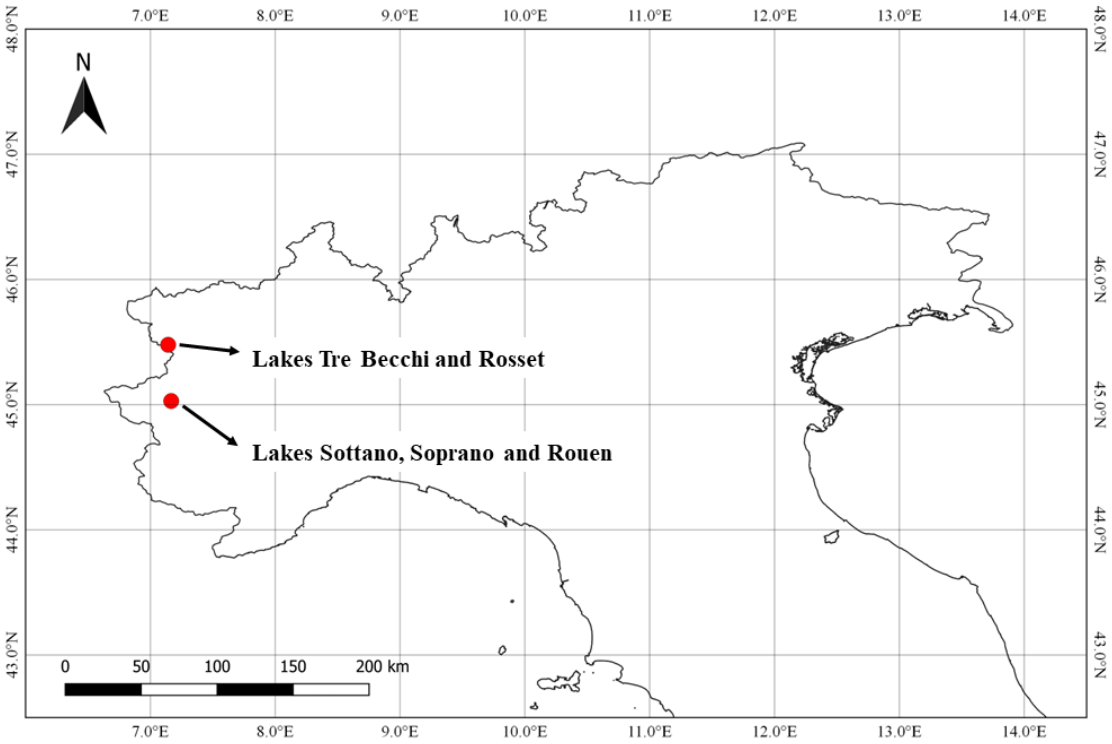

126

127 **Figure 1.** Map showing the location of the lakes under study (Piedmont region, NW Italy).

128

129 The lake water samples were preliminary characterised for dissolved organic carbon (DOC),
130 inorganic carbon (IC), and pH (see **Table S1** in the Supplementary Material, hereinafter SM). The
131 DOC was obtained as the difference between total carbon and IC, using a Shimadzu TOC-VCSH
132 instrument, based on the catalytic combustion method, and equipped with an ASI-V autosampler.
133 The pH values were measured with a Metrohm combined glass electrode (code number
134 6.0233.100).

135

136 ***Irradiation experiments***

137 Irradiation runs of lake water (80 mL) were carried out in 100 mL Duran®-glass flasks under a
138 Philips TL K05 lamp, and irradiation was mainly from the top. This lamp emits most radiation in
139 the wavelength range of 300-500 nm, with a broad band emission in the UVA region (maximum at
140 365 nm). The lamp choice is motivated by the fact that UVA is the main component of sunlight UV,

and that a very important fraction of sunlight absorption (as absorbed photon flux density) by chromophoric organic material is observed in the UVA range (Wolf et al., 2018).

At different irradiation times (between 7 and 72 h), 5- or 10-mL aliquots of lake water were withdrawn for immediate EEM or UV-Vis characterisation, respectively. Each flask (80 mL of lake water) was sampled for a maximum of two times, in order not to affect too much the solution optical path (3 cm). Therefore, each series of EEM or UV-Vis spectra referred to a given lake was obtained by independent irradiation of at least two separate aliquots of the same sample.

The spectral photon flux density of the lamp ($p^o(\lambda)$, see **Figure S1** in the SM) was obtained by combination of two techniques: *(i)* wavelength-resolved lamp emission measurements, with a calibrated Ocean Optics USB 2000 CCD spectrophotometer, and *(ii)* chemical actinometry, based on 2-nitrobenzaldehyde (2NBA) (Galbavy et al., 2010; Willett and Hites, 2000).

CCD measurement yields the raw lamp spectrum $i°(\lambda)$ on a moles-of-photons basis, which is proportional to the spectral photon flux density ($p^o(\lambda) = \vartheta\ i°(\lambda)$, where ϑ is the proportionality factor, and $p^o(\lambda)$ has units of Einstein L^{-1} s^{-1} nm^{-1}). Actinometry yields the moles of photons (Einstein units) that pass through the solution per unit volume and time, taking into account the possible reflection/scattering processes at the different interfaces (for instance, air-glass, air-water, or glass-water) (Galbavy et al., 2010). The degradation rate of 2NBA (R_{2NBA}, units of mol L^{-1} s^{-1}) can be described as follows:

$$R_{2\,NBA} = \Phi_{2\,NBA} P_{a,2\,NBA} = \Phi_{2\,NBA} \int_{\lambda} p°(\lambda)[1-10^{-A(\lambda)}]d\lambda \qquad (1)$$

where Φ_{2NBA} = 0.4 mol $Einstein^{-1}$ is the photolysis quantum yield of 2NBA (Galbavy et al., 2010), $P_{a,2NBA}$ [Einstein L^{-1} s^{-1}] the photon flux absorbed by 2NBA, and $A(\lambda)$ [unitless] the absorbance of the irradiated solution. On this basis, the factor ϑ can be obtained from known values, as follows (Carena et al., 2019):

$$\vartheta = \frac{R_{2NBA}}{\Phi_{2NBA} \int_{\lambda} i°(\lambda)[1-10^{-A(\lambda)}]d\lambda} \qquad (2)$$

To measure R_{2NBA}, aqueous solutions of 2NBA (80 mL, 80 μmol L^{-1} initial concentration) were irradiated under the lamp, and sampled (1.2 mL) after 0.5, 1, 2, 3, and 4 min. The 2NBA concentration was quantified by means of liquid chromatography (HPLC-DAD instrument; Carena et al., 2019). Then, R_{2NBA} was obtained from the 2NBA time trend, by means of the initial slope method.

EEM and UV-Vis measurements

The fluorescence excitation−emission matrix (EEM) spectra were measured with a Cary Eclipse fluorescence spectrofluorimeter, using 1-cm fluorescence quartz cuvettes. Excitation wavelengths scan was from 220 till 500 nm, with 5 nm increment steps, while emission signals were taken from 220 till 600 nm, with 1 nm steps. Slit width was 10 nm on both excitation and emission. EEM signals were normalised for the quinine sulphate unit (QSU; Fox et al., 2017). The QSU was measured from the fluorescence signal emitted at 451 nm by an acidic quinine sulphate (QS) aqueous solution (4 μg L^{-1} QS + 0.1 N H_2SO_4), after excitation at 350 nm (Fox et al., 2019).

The UV-Vis absorption spectra of the alpine lake water samples were measured with a V-550 Jasco spectrophotometer, using 5.0 cm optical path quartz cuvettes (Hellma). The absorption spectra thus obtained are reported in **Figure 2**. In some cases, absorption spectra were also measured of irradiated lake water samples, and the spectral slope S was calculated as a function of the irradiation time. To do so, the 300-345 nm spectral interval was considered for the absorption spectra, because the relevant data were well described by an exponential function (absorbance above 345 nm was often negligible, and absorbance below 300 nm was often non-exponential, see **Figure 2**):

$$A(\lambda) = A_o\, e^{-S\lambda} \qquad (3)$$

In **Eq. (3)**, $A(\lambda)$ is the absorbance at the wavelength λ, A_o is the pre-exponential term, and S is the spectral slope (Helms et al., 2008; Loiselle et al., 2009; Sharpless and Blough, 2014). The value of S was obtained by a linear least-square fit procedure of $\ln A(\lambda)$ *vs*. λ data, with A_o and S as free-floating variables.

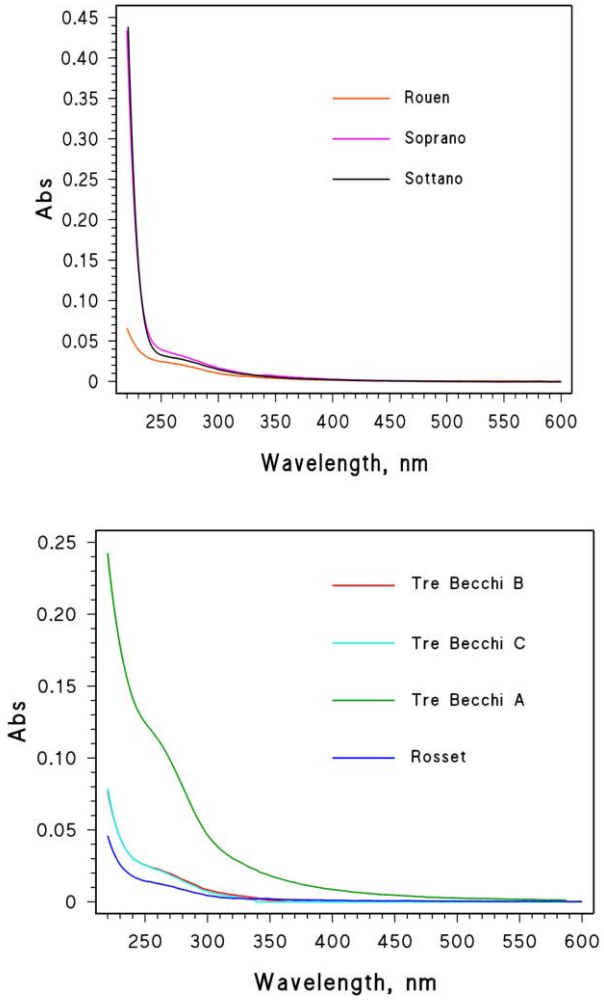

Figure 2. Absorption spectra (optical path length b = 5 cm) of the lake water samples under study.

PARAFAC Analysis

The PARAFAC analysis of the EEM spectra was carried out with the Progmeef software (http://protee.univ-tln.fr/PROGMEEF.html), with preliminary elimination of the Rayleigh and Raman scattering signals, using Zepp's method (Zepp et al., 2004). The low absorbance values of the samples (see **Figure 2**) made inner-filter correction unnecessary. PARAFAC was applied both to all the initial EEM spectra of the lake water samples and, for every lake taken separately, to each series of irradiation times. A range of 2 to 4 components was initially set, and the maximum number

of components ensuring a CONCORDIA score > 70% was chosen. In all the cases, a three-component model proved suitable to reproduce sample fluorescence.

Irradiation experiments coupled with FT-ICR MS measurements

Separate solutions of tyrosine or tryptophan (each at 0.1 mM initial concentration) were irradiated in a Pyrex glass photoreactor (130 mL volume), equipped with a 500 W Xenon lamp. The mass spectrometric measurements (FT-ICR MS: Fourier Transform-Ion Cyclotron Resonance Mass Spectrometry) of the irradiated samples, taken every 2 hours, were carried out with a Bruker 9.4 T solariX instrument (100 - 800 Da mass range; average mass resolution about 350,000 was estimated at *m/z* 319), equipped with an electro-spray ionisation (ESI) interface that was operated in negative ion mode. Further experimental details are reported as Supplementary Material, **Text S1**.

Aromaticity equivalent (*X*c) and double-bond equivalent (DBE) values were used to get insight into photodegradation product distribution. The DBE values were calculated based on **Eq. (4)**, for the elemental composition $C_cH_hO_oN_n$ obtained by FT-ICR MS (Kourtchev et al., 2016):

$$DBE = c - \frac{h}{2} + \frac{n}{2} + 1 \qquad (4)$$

where *c*, *h*, *o*, and *n* correspond to the number of carbon, hydrogen, oxygen, and nitrogen atoms in the neutral formula, respectively.

The value of *X*c, which is used to identify aromatic and polyaromatic structures in a complex mixture of compounds, was calculated as follows (Yassine et al., 2014):

$$Xc = \frac{2C+N-H-2mO}{DBE-mO} + 1 \qquad (5)$$

If DBE ≤ *m O*, or *X*c ≤ 0, it was taken *X*c = 0, where *m* is the fraction of O atoms in π-bond structures of a compound. Because of the interest in amino acid, and because ESI is sensitive to functional groups such as, for instance, carboxylic acid (R-COOH) and ester ($R\text{-}COOR_1$), we used *m* = 0.5 for the calculation of the *X*c value in this study (Wang et al., 2021; Yassine et al., 2014).

Reconstructed mass spectra were normalised to the intensity of the tyrosine (*m/z*=180.0667) and tryptophan (*m/z*=203.0826) peaks, respectively. All the formulae of the compounds were written in their neutral form to avoid confusion.

Results and Discussion

Time evolution of lake-water samples upon irradiation: EEM spectra

EEM spectra of the lake water samples were measured at different irradiation times. The fluorescence signals of the lake water evolved upon irradiation, coherently with the fact that the studied samples all showed non-negligible absorption in the UVA region (see **Figure 2**). In particular, in the case of the lakes Tre Becchi B (**Figure 3**) and Soprano (**Figure 4**), some evidence could be seen at first sight of a gradual shift in fluorescence from the protein/phenolic region (emission wavelength λ_{EM} around 325-350 nm; Stedmon et al., 2003) to the humic one (λ_{EM} around 400-450 nm; Stedmon et al., 2003), which points to photoinduced formation of HS-like fluorophores. In the other cases (Tre Becchi A, Tre Becchi C, Rosset, Rouen, Sottano, **Figures S2-S6** in SM) there was often an increase in humic-like fluorescence, without a clear trend of the signals in the protein region.

Control experiments carried out in the dark did not show significant changes in the fluorescence spectra (data not shown), which suggests that any residual biological activity in the filtered lake water samples was not able to affect fluorophores to a significant extent.

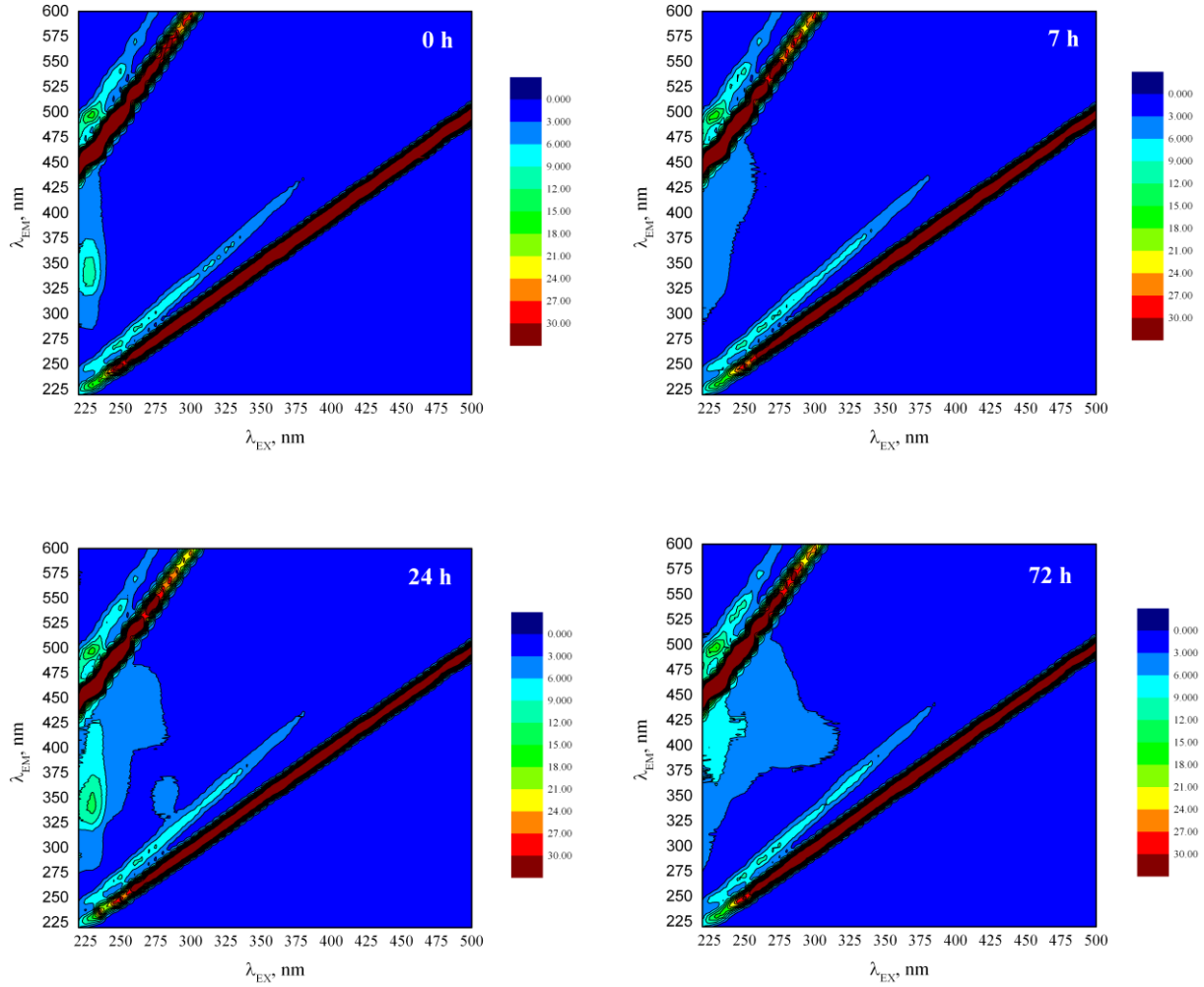

248

249
250

251 **Figure 3.** Trends of the EEM fluorescence spectra of water sampled from Lake Tre Becchi B, as a

252 function of the irradiation time. EEM signals were normalised for the quinine sulphate unit.

253

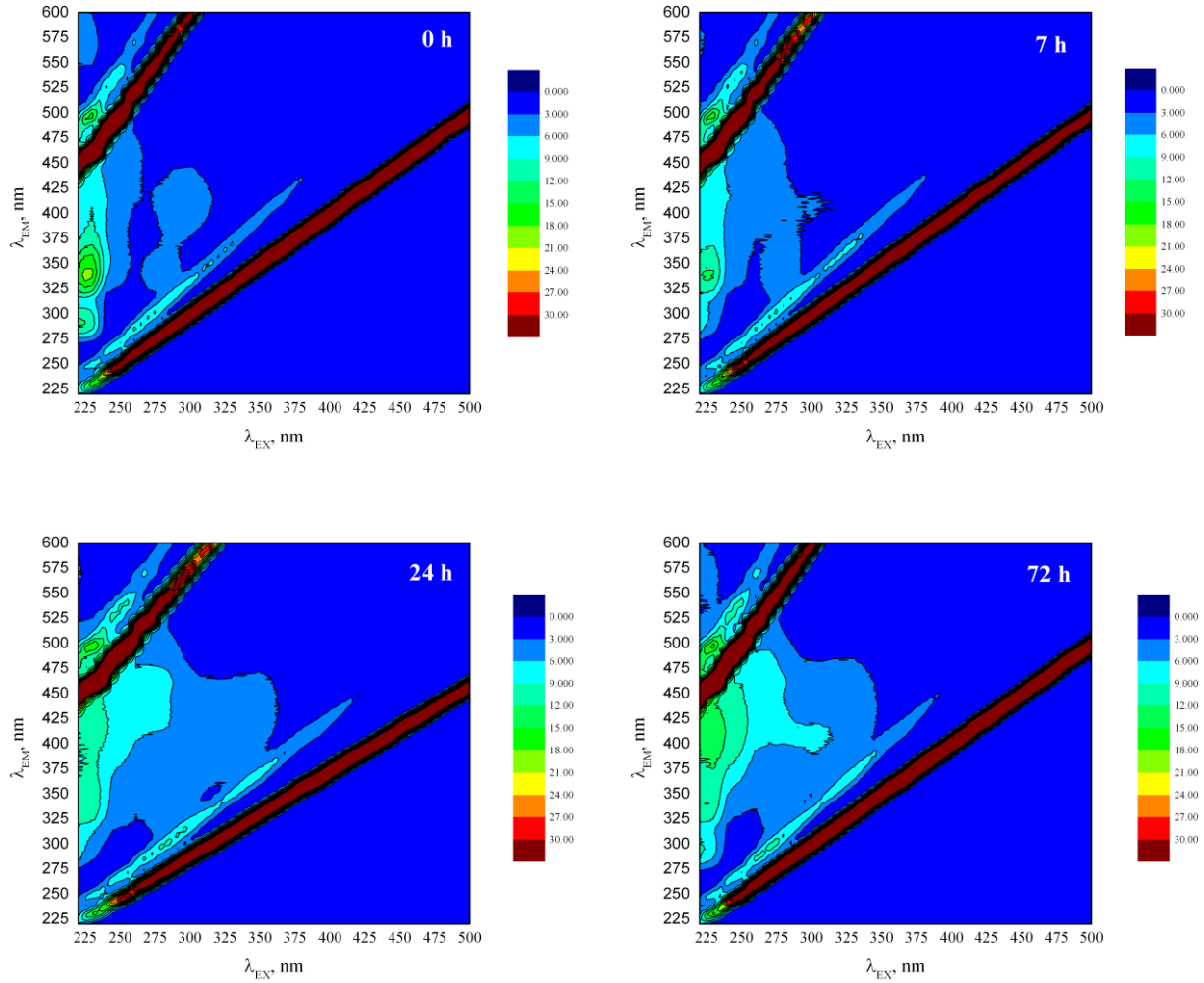

Figure 4. Trends of the EEM fluorescence spectra of water sampled from Lake Soprano, as a function of the irradiation time. EEM signals were normalised for the quinine sulphate unit.

PARAFAC analysis

PARAFAC analysis of the EEM spectra of lake water samples before irradiation showed the presence of three components (see **Figure 5**). The first had Ex/Em ~ 230/300 nm, which is usually assigned to a protein component produced by fluorescence emission of tyrosine.

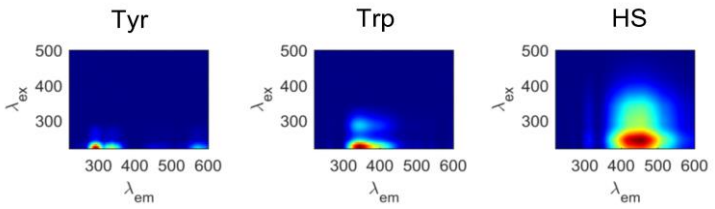

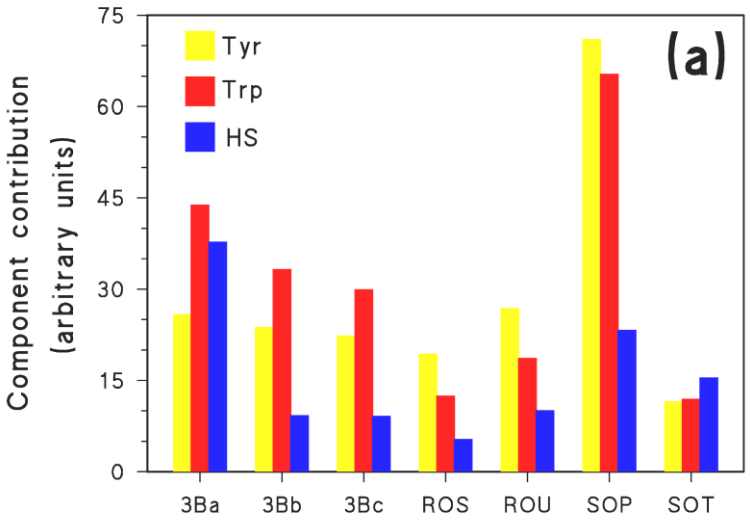

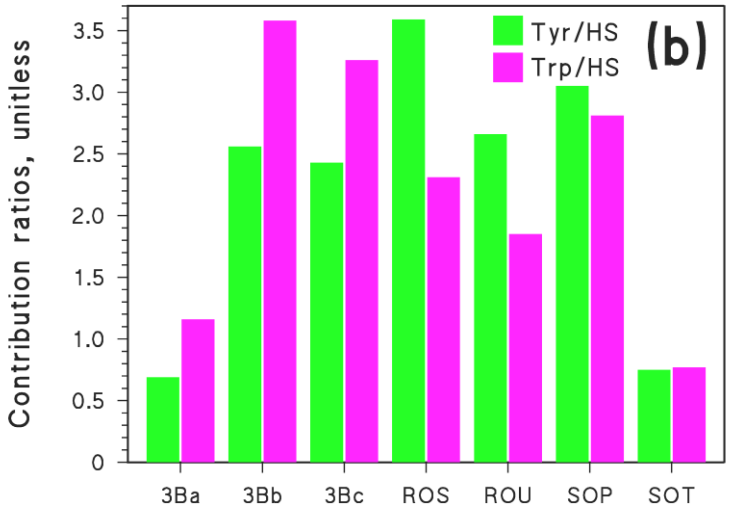

Figure 5. (a) Contributions (arbitrary units) of the three fluorescence components, found by PARAFAC analysis of EEM spectra of the investigated lake-water samples before irradiation. Component acronyms: Tyr = tyrosine-like component; Trp = tryptophan-like; HS = humic-like. The EEM traces of the three components are shown in the upper figure panel. Lake acronyms: 3Ba = Tre Becchi A; 3Bb = Tre Becchi B; 3Bc = Tre Becchi C; ROS = Rosset; Rou = Rouen; SOP = Soprano; SOT = Sottano. **(b)** Component contribution ratios, Tyr/HS and Trp/HS, in the investigated lake-water samples.

279 The second component had Ex/Em ~ 230/350 nm, which is also a protein component produced by
280 fluorescence emission of tryptophan. The third component had Ex_1/Em_1 ~ 250/450 nm and Ex_2/Em_2
281 ~ 330/450 nm, which respectively overlap with peaks A and C of humic substances. Hereinafter,
282 these three components will be labelled as Tyr, Trp, and HS, respectively. The PARAFAC
283 contributions can be related to pseudo-concentrations (arbitrary units) and give insight into the
284 fluorescence intensity of each component among the lakes. As shown in **Figure 5a**, Lake Soprano
285 (SOP) had the highest Tyr and Trp contributions, which were minimum in Lake Sottano (SOT).
286 Concerning HS, Tre Becchi A (3Ba) was the most impacted lake, followed by SOP.
287 Using the Tyr/HS and Trp/HS contribution ratios, one can compare the relative fluorophore
288 contributions under the hypothesis that fluorescence quantum yields are constant between samples.
289 **Figure 5b** shows that 3Ba and SOT were the lakes with the lowest Tyr/HS and Trp/HS contribution
290 ratios.
291 PARAFAC analysis was also applied to time series of EEM spectra, derived from irradiation
292 experiments. In particular, each time series from each irradiated lake-water sample was processed
293 separately, always finding similar components as before (Tyr, Trp, and HS). The time evolution of
294 the component contribution ratios is shown in **Figure 6** (**6a**: Tyr/HS; **6b**: Trp/HS). A decrease of
295 contribution ratio over irradiation time was observed in the case of samples from lakes Rosset
296 (ROS), Soprano (SOP), Tre Becchi B (3Bb), and Tre Becchi C (3Bc), which were also the samples
297 with the highest values of contribution ratios before irradiation. The observed decrease in the
298 Tyr/HS and Trp/HS ratios was largely due to an increase in HS fluorescence contribution, which
299 was apparent in all the samples except for Tre Becchi A (see **Figure S7** in SM). The overall results
300 warrant two observations: *(i)* there is here experimental evidence that HS-like fluorescence can be
301 produced upon irradiation of lake water samples, which in several cases led to a reduction in the
302 Tyr/HS and Trp/HS contribution ratios, and *(ii)* the phenomenon was best observed in samples
303 where initial contribution ratios were high, most likely because low HS contribution to initial
304 fluorescence minimises the impact of photobleaching on HS-like fluorescence signals.

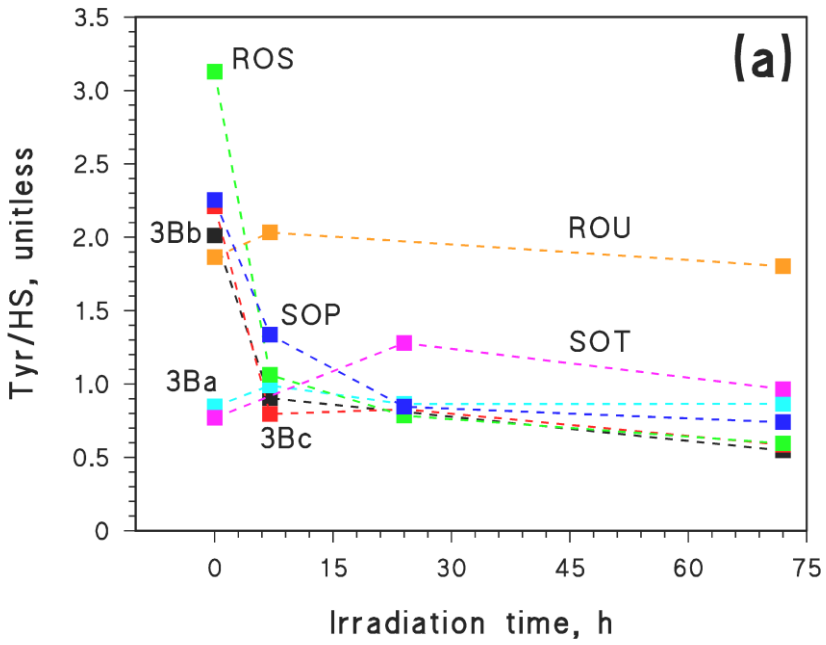

305

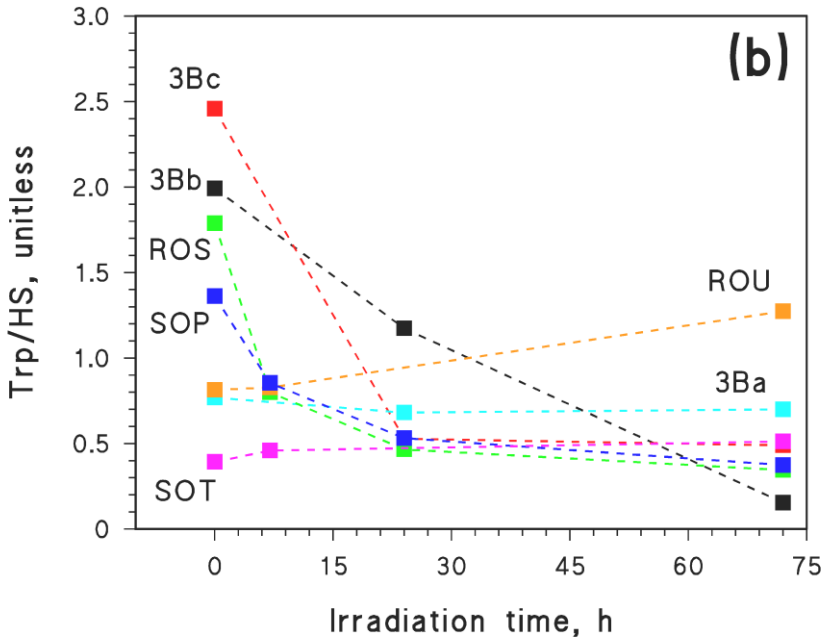

306

307

308 **Figure 6.** Time trend of the PARAFAC contribution ratios Tyr/HS **(a)** and Trp/HS **(b)**, upon UVA

309 irradiation of the lake water samples under study. Lake acronyms: 3Ba = Tre Becchi A; 3Bb = Tre

310 Becchi B; 3Bc = Tre Becchi C; ROS = Rosset; Rou = Rouen; SOP = Soprano; SOT = Sottano.

311

A decrease of Tyr/HS and Trp/HS ratio over time could be consistent with photoinduced transformation of protein-like into HS-like fluorophores (Berto et al., 2018, 2016). However, the same phenomenon could also be explained by different phenomena, such as for instance the transformation of non-fluorescent precursors into HS-like fluorophores, or an increase in fluorescence intensity of already existing fluorophores upon photoprocessing.

To corroborate evidence over the production of HS-like fluorophores, three samples (Tre Becchi B, Tre Becchi C, Soprano) were chosen for additional irradiation experiments, where the absorbance was monitored as a function of irradiation time. As shown in **Figure 7a-c**, lake-water absorbance increased upon irradiation, which is the opposite of photobleaching and indicates that photoinduced formation of chromophores took place. The same finding about increasing absorbance has already been reported in irradiation experiments of synthetic solutions, where formation of compounds with HS-like fluorescence has been observed starting from phenolic or amino-acidic precursors (Berto et al., 2016; Bianco et al., 2014).

The time evolution of the spectral slope *S* was determined in the same samples. The results reported in **Figure 7d** indicate that *S* decreased with irradiation in two out of three cases, *i.e.*, Tre Becchi B and Tre Becchi C. The spectral slope *S* is inversely correlated with the molecular mass of CDOM (Helms et al., 2008) and, in two cases, an increase in lake-water absorbance upon irradiation occurred alongside with a decrease in *S*. No significant *S* decrease was observed in the sample from Lake Soprano (**Figure 7d**), which was also the sample showing the slightest variation of absorbance upon irradiation (**Figure 7c**). These findings suggest that, in some irradiated lake water samples, increasing absorbance might be associated with an increase in the molecular mass of organic matter.

Figure 8 reports the results of FT-ICR MS measurements of irradiated tryptophan solutions, which shows the following: *(i)* The photodegradation of tryptophan produced compounds with both higher and lower molecular mass, compared to the parent molecule. In particular, for irradiation times > 2h, ~30% of the detected signals could be attributed to polyaromatic compounds (*i.e.*, compounds having more than one aromatic ring, Xc > 2.7).

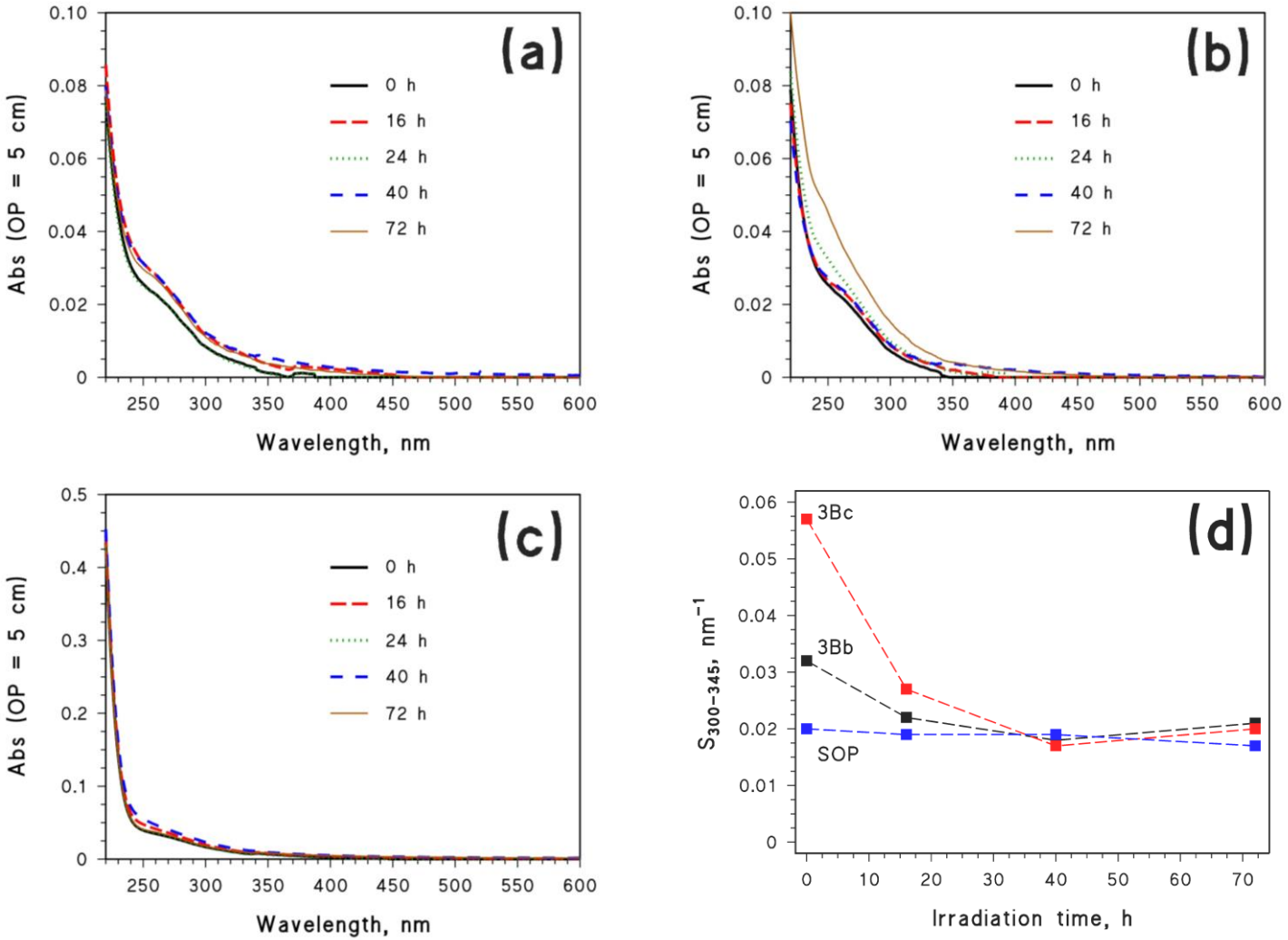

338

339

340

341 **Figure 7.** Trend of the absorbance (measured over an optical path length of 5 cm) as a function of the irradiation time, for the following lake

342 samples: **(a)** Tre Becchi B; **(b)** Tre Becchi C; **(c)** Soprano. **(d)** Time trend of the spectral slope *S* (calculated over the wavelength interval of 300-345

343 nm) for the three irradiated samples: 3Bb = Tre Becchi B; 3Bc = Tre Becchi C; SOP = Soprano.

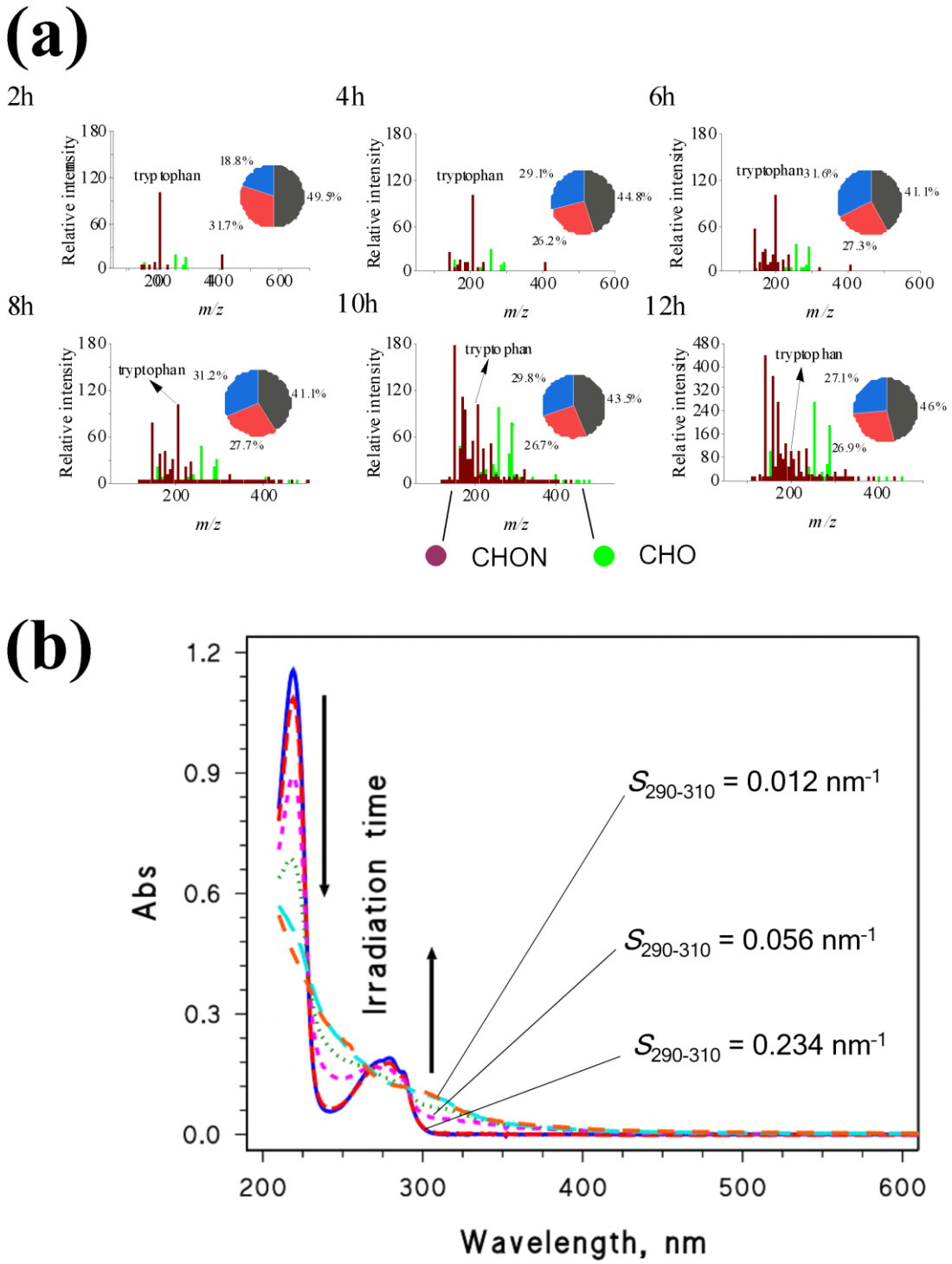

Figure 8. (a) Reconstructed mass spectra of 0-12 hours photo-degradation of 0.1 mM tryptophan, obtained by FT-ICR MS (colour code: CHON *vs.* CHO compounds). Inset pie charts show the fractions of compounds (CHO and CHON), identified by *X*c values (●: *X*c < 2.50; ●: 2.50 ≤ *X*c < 2.71; ●: *X*c ≥ 2.71). **(b)** Time evolution of the absorption spectrum of 0.1 mM tryptophan during the irradiation experiments (measured over a 1 cm optical path length, after 1:3 dilution with 10 mM phosphate buffer at pH 7). Values of the spectral slope *S*, calculated in the wavelength interval of 290-310 nm, are also highlighted.

Therefore, alongside with fragmentation, formation of larger structures was operational. *(ii)* The absorbance of the irradiated solution at $\lambda > 300$ nm increased with irradiation. *(iii)* The value of *S* decreased with irradiation in the same wavelength interval.

Based on literature reports, formation of compounds with higher molecular mass is the most likely reason of the observed spectral changes (**Figure 8**), including the increase in long-wavelength (*i.e.*, > 300 nm) absorbance, and the decrease in *S* (Berto et al., 2018; Bianco et al., 2014; Jiang et al., 2021; Smith et al., 2016). Formation of compounds with higher molecular mass was also observed in the case of tyrosine irradiation (see **Figure S8** in SM). Interestingly, parallel increases in both absorbance and molecular mass upon irradiation have also been reported in the case of environmentally significant phenolic compounds, which are also known photochemical sources of HS-like substances (Smith et al., 2016; Vione et al., 2019; Tang et al., 2020). It is possible that such processes occur in at least some of the irradiated lake water samples, and account for similar effects on the absorption spectra.

Conclusions

Here we provide evidence that irradiation is able to trigger significant formation of HS-like fluorescent compounds, in some water samples collected from mountain lakes in late summer. Fluorophore formation could be best highlighted in samples showing initial high values of protein-like vs. HS-like contribution ratios to fluorescence, as derived from PARAFAC analysis. In such samples, possible photobleaching of initially occurring HS-like fluorophores would have limited ability to interfere with photoinduced generation of further HS-like fluorescing compounds. Sample choice was probably important, as mountain lakes in late summer often show low intensity of HS-like fluorescence.

Fluorescence increase in the humic region took place alongside with an increase in sample absorbance (which is the opposite to photobleaching) and, sometimes, a decrease in spectral slope.

Both phenomena increase radiation absorption of lake water at higher wavelengths. This event has potential ecologic significance, because radiation-absorbing compounds screen biologically harmful UV radiation. Therefore, photoinduced chromophore formation in otherwise clear water environments might play a role in decreasing UV stress to living organisms, and the interplay between this phenomenon and photobleaching (likely taking place at the same time) will require further investigation.

The origin of the fluorescence increase will also require further investigation. Photochemical precursors of HS-like substances (tyrosine, tryptophan, and several phenols) are all able to produce compounds with higher molecular mass when irradiated, which also leads to an increase in long-wavelength absorbance. Such a scenario, though reasonable, still has to be conclusively demonstrated.

Acknowledgements

L.C. and D.V. wish to thank Dr. S. Bertinetti and Mr. L. Rapa for their help during lake-water sampling. L.C. acknowledges Compagnia di San Paolo (Torino, Italy) for financially supporting his PhD fellowship. The stay of D.V. in Toulon was financially supported by invited research call 2021.

References

Andersen, C.M., Bro, R., 2003. Practical aspects of PARAFAC modeling of fluorescence excitation-emission data. J. Chemom. 17, 200–215. https://doi.org/https://doi.org/10.1002/cem.790

Berg, S.M., Whiting, Q.T., Herrli, J.A., Winkels, R., Wammer, K.H., Remucal, C.K., 2019. The Role of Dissolved Organic Matter Composition in Determining Photochemical Reactivity at the Molecular Level. Environ. Sci. Technol. 53, 11725–11734. https://doi.org/10.1021/acs.est.9b03007

Berto, S., De Laurentiis, E., Scapuzzi, C., Chiavazza, E., Corazzari, I., Turci, F., Minella, M., Buscaino, R., Daniele, P.G., Vione, D., 2018. Phototransformation of l-tryptophan and formation of humic substances in water. Environ. Chem. Lett. 16, 1035–1041. https://doi.org/10.1007/s10311-018-0714-y

Berto, S., De Laurentiis, E., Tota, T., Chiavazza, E., Daniele, P.G., Minella, M., Isaia, M., Brigante, M., Vione, D., 2016. Properties of the humic-like material arising from the photo-transformation of l-tyrosine. Sci. Total Environ. 545–546, 434–444. https://doi.org/https://doi.org/10.1016/j.scitotenv.2015.12.047

Bianco, A., 2013. Abiotic photosynthesis of humic and fulvic acids from compounds that commonly occur in natural waters. MSc thesis (in Italian), University of Torino.

Bianco, A., Minella, M., De Laurentiis, E., Maurino, V., Minero, C., Vione, D., 2014. Photochemical generation of photoactive compounds with fulvic-like and humic-like fluorescence in aqueous solution. Chemosphere 111, 529–536. https://doi.org/https://doi.org/10.1016/j.chemosphere.2014.04.035

Bridgeman, J., Bieroza, M., Baker, A., 2011. The application of fluorescence spectroscopy to organic matter characterisation in drinking water treatment. Rev. Environ. Sci. Bio/Technology 10, 277. https://doi.org/10.1007/s11157-011-9243-x

Brinkmann, T., Sartorius, D., Frimmel, F.H., 2003. Photobleaching of humic rich dissolved organic matter. Aquat. Sci. 65, 415–424. https://doi.org/10.1007/s00027-003-0670-9

Bro, R., 1997. PARAFAC. Tutorial and applications. Chemom. Intell. Lab. Syst. 38, 149–171. https://doi.org/https://doi.org/10.1016/S0169-7439(97)00032-4

Carena, L., Puscasu, C.G., Comis, S., Sarakha, M., Vione, D., 2019. Environmental photodegradation of emerging contaminants: A re-examination of the importance of triplet-sensitised processes, based on the use of 4-carboxybenzophenone as proxy for the chromophoric dissolved organic matter. Chemosphere 237, 124476. https://doi.org/10.1016/j.chemosphere.2019.124476

Clark, J.B., Neale, P., Tzortziou, M., Cao, F., Hood, R.R., 2019. A mechanistic model of photochemical transformation and degradation of colored dissolved organic matter. Mar. Chem. 214, 103666. https://doi.org/https://doi.org/10.1016/j.marchem.2019.103666

Coble, P.G., 1996. Characterization of marine and terrestrial DOM in seawater using excitation-emission matrix spectroscopy. Mar. Chem. 51, 325–346. https://doi.org/https://doi.org/10.1016/0304-4203(95)00062-3

Cory, R.M., McKnight, D.M., 2005. Fluorescence Spectroscopy Reveals Ubiquitous Presence of Oxidized and Reduced Quinones in Dissolved Organic Matter. Environ. Sci. Technol. 39, 8142–8149. https://doi.org/10.1021/es0506962

Dainard, P.G., Gueguen, C., McDonald, N., Williams, W.J., 2015. Photobleaching of fluorescent dissolved organic matter in Beaufort Sea and North Atlantic Subtropical Gyre. Mar. Chem. 177, 630–637. https://doi.org/10.1016/j.marchem.2015.10.004

De Laurentiis, E., Minella, M., Maurino, V., Minero, C., Brigante, M., Mailhot, G., Vione, D., 2012. Photochemical production of organic matter triplet states in water samples from mountain lakes, located below or above the tree line. Chemosphere 88, 1208–1213. https://doi.org/https://doi.org/10.1016/j.chemosphere.2012.03.071

De Laurentiis, E., Sur, B., Pazzi, M., Maurino, V., Minero, C., Mailhot, G., Brigante, M., Vione, D., 2013. Phenol transformation and dimerisation, photosensitised by the triplet state of 1-nitronaphthalene: A possible pathway to humic-like substances (HULIS) in atmospheric waters. Atmos. Environ. 70, 318–327. https://doi.org/https://doi.org/10.1016/j.atmosenv.2013.01.014

De Paolis, F., Kukkonen, J., 1997. Binding of organic pollutants to humic and fulvic acids: Influence of pH and the structure of humic material. Chemosphere 34, 1693–1704. https://doi.org/https://doi.org/10.1016/S0045-6535(97)00026-X

Del Vecchio, R., Blough, N. V, 2002. Photobleaching of chromophoric dissolved organic matter in natural waters: kinetics and modeling. Mar. Chem. 78, 231–253. https://doi.org/https://doi.org/10.1016/S0304-4203(02)00036-1

Fox, B.G., Thorn, R.M.S., Anesio, A.M., Cox, T., Attridge, J.W., Reynolds, D.M., 2019. Microbial Processing and Production of Aquatic Fluorescent Organic Matter in a Model Freshwater System. Water. https://doi.org/10.3390/w11010010

Fox, B.G., Thorn, R.M.S., Anesio, A.M., Reynolds, D.M., 2017. The in situ bacterial production of fluorescent organic matter; an investigation at a species level. Water Res. 125, 350–359. https://doi.org/https://doi.org/10.1016/j.watres.2017.08.040

Galbavy, E.S., Ram, K., Anastasio, C., 2010. Chemistry 2-Nitrobenzaldehyde as a chemical

actinometer for solution and ice photochemistry. J. Photochem. Photobiol. A Chem. 209, 186–192. https://doi.org/10.1016/j.jphotochem.2009.11.013

Galgani, L., Tognazzi, A., Rossi, C., Ricci, M., Angel Galvez, J., Dattilo, A.M., Cozar, A., Bracchini, L., Loiselle, S.A., 2011. Assessing the optical changes in dissolved organic matter in humic lakes by spectral slope distributions. J. Photochem. Photobiol. B Biol. 102, 132–139. https://doi.org/https://doi.org/10.1016/j.jphotobiol.2010.10.001

Gu, Y., Lensu, A., Perämäki, S., Ojala, A., Vähätalo, A. V, 2017. Iron and pH Regulating the Photochemical Mineralization of Dissolved Organic Carbon. ACS Omega 2, 1905–1914. https://doi.org/10.1021/acsomega.7b00453

He, W., Choi, I., Lee, J.-J., Hur, J., 2016. Coupling effects of abiotic and biotic factors on molecular composition of dissolved organic matter in a freshwater wetland. Sci. Total Environ. 544, 525–534. https://doi.org/https://doi.org/10.1016/j.scitotenv.2015.12.008

Helms, J.R., Mao, J., Stubbins, A., Schmidt-Rohr, K., Spencer, R.G.M., Hernes, P.J., Mopper, K., 2014. Loss of optical and molecular indicators of terrigenous dissolved organic matter during long-term photobleaching. Aquat. Sci. 76, 353–373. https://doi.org/10.1007/s00027-014-0340-0

Helms, J.R., Stubbins, A., Ritchie, J.D., Minor, E.C., Kieber, D.J., Mopper, K., 2008. Absorption spectral slopes and slope ratios as indicators of molecular weight, source, and photobleaching of chromophoric dissolved organic matter. Limnol. Oceanogr. 53, 955–969. https://doi.org/https://doi.org/10.4319/lo.2008.53.3.0955

Hoffer, A., Kiss, G., Blazsó, M., Gelencsér, A., 2004. Chemical characterization of humic-like substances (HULIS) formed from a lignin-type precursor in model cloud water. Geophys. Res. Lett. 31. https://doi.org/https://doi.org/10.1029/2003GL018962

Jiang, W., Misovich, M. V, Hettiyadura, A.P.S., Laskin, A., McFall, A.S., Anastasio, C., Zhang, Q., 2021. Photosensitized Reactions of a Phenolic Carbonyl from Wood Combustion in the Aqueous Phase—Chemical Evolution and Light Absorption Properties of AqSOA. Environ. Sci. Technol. 55, 5199–5211. https://doi.org/10.1021/acs.est.0c07581

Koukal, B., Guéguen, C., Pardos, M., Dominik, J., 2003. Influence of humic substances on the toxic effects of cadmium and zinc to the green alga Pseudokirchneriella subcapitata. Chemosphere 53, 953–961. https://doi.org/https://doi.org/10.1016/S0045-6535(03)00720-3

Kourtchev, I., Godoi, R.H.M., Connors, S., Levine, J.G., Archibald, A.T., Godoi, A.F.L., Paralovo, S.L., Barbosa, C.G.G., Souza, R.A.F., Manzi, A.O., Seco, R., Sjostedt, S., Park, J.-H., Guenther, A., Kim, S., Smith, J., Martin, S.T., Kalberer, M., 2016. Molecular composition of organic aerosols in central Amazonia: an ultra-high-resolution mass spectrometry study.

Atmos. Chem. Phys. 16, 11899–11913. https://doi.org/10.5194/acp-16-11899-2016
Krachler, R., Krachler, R.F., 2021. Northern High-Latitude Organic Soils As a Vital Source of River-Borne Dissolved Iron to the Ocean. Environ. Sci. Technol. 55, 9672–9690. https://doi.org/10.1021/acs.est.1c01439
Loiselle, S.A., Bracchini, L., Dattilo, A.M., Ricci, M., Tognazzi, A., Cózar, A., Rossi, C., 2009. The optical characterization of chromophoric dissolved organic matter using wavelength distribution of absorption spectral slopes. Limnol. Oceanogr. 54, 590–597. https://doi.org/https://doi.org/10.4319/lo.2009.54.2.0590
Mabato, B.R.G., Lyu, Y., Ji, Y., Li, Y.J., Huang, D.D., Li, X., Nah, T., Lam, C.H., Chan, C.K., 2022. Aqueous secondary organic aerosol formation from the direct photosensitized oxidation of vanillin in the absence and presence of ammonium nitrate. Atmos. Chem. Phys. 22, 273–293. https://doi.org/10.5194/acp-22-273-2022
Minor, E.C., Swenson, M.M., Mattson, B.M., Oyler, A.R., 2014. Structural characterization of dissolved organic matter: a review of current techniques for isolation and analysis. Environ. Sci. Process. Impacts 16, 2064–2079. https://doi.org/10.1039/C4EM00062E
Murphy, K.R., Stedmon, C.A., Graeber, D., Bro, R., 2013. Fluorescence spectroscopy and multi-way techniques. PARAFAC. Anal. Methods 5, 6557–6566. https://doi.org/10.1039/C3AY41160E
Nelson, N.B., Siegel, D.A., 2013. The Global Distribution and Dynamics of Chromophoric Dissolved Organic Matter. Ann. Rev. Mar. Sci. 5, 447–476. https://doi.org/10.1146/annurev-marine-120710-100751
Nguyen, H.V.-M., Lee, M.-H., Hur, J., Schlautman, M.A., 2013. Variations in spectroscopic characteristics and disinfection byproduct formation potentials of dissolved organic matter for two contrasting storm events. J. Hydrol. 481, 132–142. https://doi.org/https://doi.org/10.1016/j.jhydrol.2012.12.044
Niu, X.-Z., Liu, C., Gutierrez, L., Croué, J.-P., 2014. Photobleaching-induced changes in photosensitizing properties of dissolved organic matter. Water Res. 66, 140–148. https://doi.org/https://doi.org/10.1016/j.watres.2014.08.017
Osburn, C.L., Stedmon, C.A., 2011. Linking the chemical and optical properties of dissolved organic matter in the Baltic–North Sea transition zone to differentiate three allochthonous inputs. Mar. Chem. 126, 281–294. https://doi.org/https://doi.org/10.1016/j.marchem.2011.06.007
Remucal, C.K., 2014. The role of indirect photochemical degradation in the environmental fate of pesticides: a review. Environ. Sci. Process. Impacts 16, 628–653.

https://doi.org/10.1039/c3em00549f
Shank, G.C., Zepp, R.G., Vähätalo, A., Lee, R., Bartels, E., 2010. Photobleaching kinetics of chromophoric dissolved organic matter derived from mangrove leaf litter and floating Sargassum colonies. Mar. Chem. 119, 162–171. https://doi.org/https://doi.org/10.1016/j.marchem.2010.01.003
Sharpless, C.M., Blough, N. V, 2014. The importance of charge-transfer interactions in determining chromophoric dissolved organic matter (CDOM) optical and photochemical properties. Environ. Sci. Process. Impacts 16, 654–671. https://doi.org/10.1039/c3em00573a
Smith, J.D., Kinney, H., Anastasio, C., 2016. Phenolic carbonyls undergo rapid aqueous photodegradation to form low-volatility, light-absorbing products. Atmos. Environ. 126, 36–44. https://doi.org/https://doi.org/10.1016/j.atmosenv.2015.11.035
Sommaruga, R., 2001. The role of solar UV radiation in the ecology of alpine lakes. J. Photochem. Photobiol. B Biol. 62, 35–42. https://doi.org/https://doi.org/10.1016/S1011-1344(01)00154-3
Sommaruga, R., Psenner, R., Schafferer, E., Koinig, K.A., Sommaruga-Wögrath, S., 1999. Dissolved Organic Carbon Concentration and Phytoplankton Biomass in High-Mountain Lakes of the Austrian Alps: Potential Effect of Climatic Warming on UV Underwater Attenuation. Arctic, Antarct. Alp. Res. 31, 247–253. https://doi.org/https://doi.org/10.1080/15230430.1999.12003305
Stedmon, C.A., Markager, S., Bro, R., 2003. Tracing dissolved organic matter in aquatic environments using a new approach to fluorescence spectroscopy. Mar. Chem. 82, 239–254. https://doi.org/https://doi.org/10.1016/S0304-4203(03)00072-0
Suzuki, D., Shoji, R., 2020. Toxicological effects of chlorophenols to green algae observed at various pH and concentration of humic acid. J. Hazard. Mater. 400, 123079. https://doi.org/https://doi.org/10.1016/j.jhazmat.2020.123079
Tang, S., Li, F., Tsona, N.T., Lu, C., Wang, X., Du, L., 2020. Aqueous-Phase Photooxidation of Vanillic Acid: A Potential Source of Humic-Like Substances (HULIS). ACS Earth Sp. Chem. 4, 862–872. https://doi.org/10.1021/acsearthspacechem.0c00070
Tipping, E., Woof, C., Rigg, E., Harrison, A.F., Ineson, P., Taylor, K., Benham, D., Poskitt, J., Rowland, A.P., Bol, R., Harkness, D.D., 1999. Climatic influences on the leaching of dissolved organic matter from upland UK moorland soils, investigated by a field manipulation experiment. Environ. Int. 25, 83–95. https://doi.org/https://doi.org/10.1016/S0160-4120(98)00098-1
Trubetskaya, O.E., Richard, C., Trubetskoj, O.A., 2016. High amounts of free aromatic amino acids in the protein-like fluorescence of water-dissolved organic matter. Environ. Chem. Lett. 14,

495–500. https://doi.org/10.1007/s10311-016-0556-4

Vähätalo, A. V, Wetzel, R.G., 2004. Photochemical and microbial decomposition of chromophoric dissolved organic matter during long (months–years) exposures. Mar. Chem. 89, 313–326. https://doi.org/https://doi.org/10.1016/j.marchem.2004.03.010

Vione, D., Minella, M., Maurino, V., Minero, C., 2014. Indirect Photochemistry in Sunlit Surface Waters: Photoinduced Production of Reactive Transient Species. Chem. Eur. J. 20, 10590–10606. https://doi.org/10.1002/chem.201400413

Vione, D., Albinet, A., Barsotti, F., Mekic, M., Jiang, B., Minero, C., Brigante, M., Gligorovski, S., 2019. Formation of substances with humic-like fluorescence properties, upon photoinduced oligomerization of typical phenolic compounds emitted by biomass burning, Atmos. Environ. 206, 197-207. https://doi.org/10.1016/j.atmosenv.2019.03.005

Vione, D., Minero, C., Carena, L., 2021. Fluorophores in surface freshwaters: importance, likely structures, and possible impacts of climate change. Environ. Sci. Process. Impacts 23, 1429–1442. https://doi.org/10.1039/D1EM00273B

Wang, Y., Mekic, M., Li, P., Deng, H., Liu, S., Jiang, B., Jin, B., Vione, D., Gligorovski, S., 2021. Ionic Strength Effect Triggers Brown Carbon Formation through Heterogeneous Ozone Processing of Ortho-Vanillin. Environ. Sci. Technol. 55, 4553–4564. https://doi.org/10.1021/acs.est.1c00874

Willett, K.L., Hites, R.A., 2000. Chemical Actinometry : Using o-Nitrobenzaldehyde to Measure Light Intensity in Photochemical Experiments. J. Chem. Educ. 77, 900–902. https://doi.org/https://doi.org/10.1021/ed077p900

Wolf, R., Thrane, J.-E., Hessen, D.O., Andersen, T., 2018. Modelling ROS formation in boreal lakes from interactions between dissolved organic matter and absorbed solar photon flux. Water Res. 132, 331–339. https://doi.org/https://doi.org/10.1016/j.watres.2018.01.025

Worms, I.A.M., Adenmatten, D., Miéville, P., Traber, J., Slaveykova, V.I., 2015. Photo-transformation of pedogenic humic acid and consequences for Cd(II), Cu(II) and Pb(II) speciation and bioavailability to green microalga. Chemosphere 138, 908–915. https://doi.org/https://doi.org/10.1016/j.chemosphere.2014.10.093

Yamashita, Y., Nosaka, Y., Suzuki, K., Ogawa, H., Takahashi, K., Saito, H., 2013. Photobleaching as a factor controlling spectral characteristics of chromophoric dissolved organic matter in open ocean. Biogeosciences 10, 7207–7217. https://doi.org/10.5194/bg-10-7207-2013

Yang, X., Yuan, J., Yue, F.-J., Li, S.-L., Wang, B., Mohinuzzaman, M., Liu, Y., Senesi, N., Lao, X., Li, L., Liu, C.-Q., Ellam, R.M., Vione, D., Mostofa, K.M.G., 2021. New insights into mechanisms of sunlight- and dark-mediated high-temperature accelerated diurnal production-

601 degradation of fluorescent DOM in lake waters. Sci. Total Environ. 760, 143377.
602 https://doi.org/https://doi.org/10.1016/j.scitotenv.2020.143377
603 Yassine, M.M., Harir, M., Dabek-Zlotorzynska, E., Schmitt-Kopplin, P., 2014. Structural
604 characterization of organic aerosol using Fourier transform ion cyclotron resonance mass
605 spectrometry: Aromaticity equivalent approach. Rapid Commun. Mass Spectrom. 28, 2445–
606 2454. https://doi.org/https://doi.org/10.1002/rcm.7038
607 Zepp, R.G., Sheldon, W.M., Moran, M.A., 2004. Dissolved organic fluorophores in southeastern
608 US coastal waters: correction method for eliminating Rayleigh and Raman scattering peaks in
609 excitation–emission matrices. Mar. Chem. 89, 15–36.
610 https://doi.org/https://doi.org/10.1016/j.marchem.2004.02.006
611 Zhang, D., Yan, S., Song, W., 2014. Photochemically induced formation of reactive oxygen species
612 (ROS) from effluent organic matter. Environ. Sci. Technol. 48, 12645-12653.
613 Zhou, L., Sleiman, M., Fine, L., Ferronato, C., de Sainte Claire, P., Vulliet, E., Chovelon, J.-M.,
614 Xiu, G., Richard, C., 2019. Contrasting photoreactivity of β2-adrenoceptor agonists
615 Salbutamol and Terbutaline in the presence of humic substances. Chemosphere 228, 9–16.
616 https://doi.org/https://doi.org/10.1016/j.chemosphere.2019.04.104
617